ELSEVIER

Cardiovascular Research 44 (1999) 121–131

Cardiovascular Research

www.elsevier.com/locate/cardiores
www.elsevier.nl/locate/cardiores

Ionic mechanisms of electrical remodeling in human atrial fibrillation

Ralph F. Bosch*, Xiaorong Zeng, Joachim B. Grammer, Katarina Popovic, Christian Mewis, Volker Kühlkamp

Department of Cardiology, University of Tübingen, Tübingen, Germany

Received 15 February 1999; accepted 23 April 1999

Abstract

Objectives: Atrial fibrillation (AF) is associated with a decrease in atrial ERP and ERP adaptation to rate as well as changes in atrial conduction velocity. The cellular changes in repolarization and the underlying ionic mechanisms in human AF are only poorly understood. **Methods:** Action potentials (AP) and ionic currents were studied with the patch clamp technique in single atrial myocytes from patients in chronic AF and compared to those from patients in stable sinus rhythm (SR). **Results:** The presence of AF was associated with a marked shortening of the AP duration and a decreased rate response of atrial repolarization. L-type calcium current ($I_{Ca,L}$) and the transient outward current (I_{to}) were both reduced about 70% in AF, whereas an increased steady-state outward current was detectable at test potentials between −30 and 0 mV. The inward rectifier potassium current (I_{K1}) and the acetylcholine-activated potassium current (I_{KACh}) were increased in AF at hyperpolarizing potentials. Voltage-dependent inactivation of the fast sodium current (I_{Na}) was shifted to more positive voltages in AF. **Conclusions:** AF in humans leads to important changes in atrial potassium and calcium currents that likely contribute to the decrease in APD and APD rate adaptation. These changes contribute to electrical remodeling in AF and are therefore important factors for the perpetuation of the arrhythmia.

Keywords: Experimental; Heart; Cellular; Electrophysiology; Arrhythmia (mechanisms); Ca-channel; K-channel; Na-channel; Ion channels

This article is referred to in the Editorial by M.A. Alessie (pages 10–12) in this issue.

1. Introduction

Atrial fibrillation (AF) is the most common arrhythmia in man and its prevalence will increase with the aging of the population [1–3]. The presence of AF is associated with a considerable increase in morbidity [4,5] and in mortality [1,6]. In recent years, the functional mechanisms underlying AF have been investigated in animal models [7–10] and in humans [11–14]. From these studies, it became evident that AF is characterized by a marked decrease in the atrial ERP and in ERP adaptation to rate [7–14] as well as a decrease in atrial conduction velocity [9,12], thereby favoring the occurrence of multiple-wavelet reentry [15]. Little information is available about the ionic mechanisms underlying AF in humans. In the canine rapid pacing model of AF, Yue et al. [16] have demonstrated a decrease in $I_{Ca,L}$ and in I_{to} as factors underlying AP shortening. In that model, a decreased I_{Na} was observed in AF that correlated with the slowing of atrial conduction [17]. The only study in humans reported a decrease in I_{to} and I_{sus} as well as an increase in I_{K1} in left but not in right atrial myocytes in chronic AF [18]. At the moment, no data are available upon the effects of human AF on repolarization on a cellular level, on inward currents like $I_{Ca,L}$ and I_{Na}, and only limited information is available on potassium currents. The purpose of the present study therefore was to study the effects of AF on AP in isolated myocytes, and to characterize the changes in potassium

*Corresponding author. Tel.: +49-7071-298-3196; fax: +49-7071-295-285.

E-mail address: ralph.bosch@uni-tuebingen.de (R.F. Bosch)

Time for primary review 16 days.

0008-6363/99/$ – see front matter
PII: S0008-6363(99)00178-9

currents (I_{to} [19]; I_{sus} (I_{Kur}) [20,21]; I_{K1} [22]; I_{KACh} [23]), calcium – ($I_{Ca,L}$) and sodium currents (I_{Na}) that underlie altered repolarization.

2. Methods

2.1. Patients' characteristics and isolation of single atrial cells

Right atrial appendages were obtained at the time of cardiac surgery by following procedures approved by the institutional review committee. The investigation conforms with the principles outlined in the Declaration of Helsinki. 17 patients were assigned to the SR group and 8 to the chronic AF group according to the underlying cardiac rhythm. Chronic AF was defined as permanent AF of at least 1 month duration, patients with paroxysmal AF were not included in the study. Patients' characteristics are listed in Table 1. Single myocytes were isolated by enzymatic dissociation with the chunk method as previously described [24]. The specimens were transported to the laboratory in a nominally Ca^{2+}-free cardioplegic solution (100% O_2, room temperature) containing (mM) KH_2PO_4 50, $MgSO_4$ 8, Adenosine 5, HEPES 10, Glucose 140, Mannitol 100, Taurine 10, pH was adjusted to 7.4 with KOH. Chunks were washed in 25 ml EGTA solution containing (mM) NaCl 137, KH_2PO_4 5, $MgSO_4$ 1, Glucose 10, HEPES 5, Taurine 10, EGTA 0.1, pH was adjusted to 7.4 with NaOH. After washout of blood and calcium, the chunks were incubated for 35 min in 5 ml Ca^{2+}-free Enzyme Incubation Medium (EIM) with the addition of 150 U/ml collagenase (Type V, Sigma), 12.6 U/ml protease (Type XXIV, Sigma) and 1 mg/ml albumin (Sigma). The EIM solution contained (mM) NaCl 137, KH_2PO_4 5, $MgSO_4$ 1, Glucose 10, HEPES 5, Taurine 10, pH 7.4 (adjusted with NaOH). The EIM was maintained at 35°C and continuously gassed with 100% O_2. This period of digestion was followed by a 1 min wash in EIM solution without any enzymes. Subsequently, the supernatant was removed and replaced by a fresh enzyme medium with the same composition but without protease until rod-shaped cells were present. Cells were kept in a ''Kraftbruehe'' storage solution containing (mM) KCl 20,

Table 1
Patients' characteristics

	Sinus rhythm	Atrial fibrillation
n (m/f)	17 (15/2)	8 (6/2)
Age (Mean±SD)	62±8	69±4
Cardiac disease		
Coronary artery disease	16	4
Mitral valve disease	0	2
Aortic valve disease	1	2
Left ventricular function		
Normal	9	5
Mild reduction	2	0
Moderate reduction	1	1
Severe reduction	2	2
Not available	3	0
Left atrial size		
Normal	5	0
Mild dilation	2	0
Moderate dilation	0	4
Severe dilation	2	1
Not available	8	3
Drugs		
β-blockers	11 (65%)	2 (25%)
Ca-channel blockers (non-dihydropyridines)	1 (6%)	1 (13%)
Ca-channel blockers (dihydropyridines)	1 (6%)	1 (13%)
Sotalol	0 (0%)	1 (13%)
ACE-Inhibitors	4 (24%)	4 (50%)
Digitalis	2 (12%)	8 (100%)
Diuretics	5 (29%)	5 (63%)
Nitrates	11 (65%)	1 (13%)

KH_2PO_4 10, Glucose 25, Mannitol 5, Albumin 1, L-Glutamic acid 70, β-hydroxybutyrate 10, Taurine 10, EGTA 10, pH 7.4 (adjusted with KOH).

2.2. Patch clamp technique

Only quiescent, rod-shaped cells with clear cross striations were studied. Ionic currents were recorded using the whole cell configuration of the voltage clamp technique. Borosilicate glass electrodes (outer diameter 1.0 mm) with resistances of around 1 MΩ to record I_{Na} and 3 to 5 MΩ for recording of action potentials and other ionic currents were connected to a patch clamp amplifier (Axopatch 200B, Axon Instruments). Data were sampled with an A/D converter (Digidata 1200, Axon Instruments) and stored for subsequent analysis. The sampling frequency depended on the recording interval, with a frequency of 10 kHz used for rapidly changing currents and frequencies as low as 0.4 kHz used for long recordings of slowly changing currents. Recordings were low-pass filtered at 2 kHz. Tip potentials were zeroed before formation of the pipette-membrane seal. After rupture of the cell membrane, pipette series resistance (R_s) was electrically compensated to minimize the capacitive surge on the current recording and the voltage drop across the clamped membrane. R_s was calculated by dividing the capacitive time constant, obtained by fitting the decay of the capacitive transient before and after compensation, by the calculated membrane capacitance (the time integral of the capacitive response to a 5 mV hyperpolarizing pulse from a holding potential of −60 mV, divided by the voltage drop). Membrane capacitance was identical in the 2 groups: 72.1±3.0 pA/pF (n=167) in SR and 76.6±4.8 pA/pF (n=78) in AF; p=ns vs. SR. To control for differences in cell size, all mean current data are expressed as current densities (i.e., normalized to capacitance). Before compensation, R_s averaged 7.8±0.2 and 9.6±0.4 MΩ in the SR and AF group, and the capacitive time constants were 537±23 and 671±35 μs, respectively. Corresponding values for R_s after compensation were 3.2±0.3 and 3.1±0.2 MΩ, and 246±11 and 264±11 μs for the capacitive time constants. For recording I_{Na}, great care was taken to minimize the voltage drop across the R_s. This included the selection of small cells and of low resistance electrodes. R_s in these cells averaged 3.9±0.3 MΩ and 1.94±0.14 MΩ before and after compensation. Cells with a voltage drop of >7 mV were rejected, the mean voltage drop of the cells included was 4.88±0.26 mV. The compositions of the bath and pipette solutions are listed in Table 2. For the recording of potassium currents, $I_{Ca,L}$ was blocked with 1 μmol/l nisoldipine [14,25]. I_{Na} was recorded at room temperature, all other experiment were conducted at 36°C.

2.3. Data analysis

Group data are expressed as mean±SE. Comparisons between SR and AF groups were made using a Student's non-paired t-test. Differences with a two-tailed p value< 0.05 were considered statistically significant. A nonlinear least-square curve-fitting program (CLAMPFIT in pCLAMP 6.0 or Sigma Plot) was used to perform curve fitting procedures.

3. Results

3.1. Effects of chronic AF on action potentials

AP were recorded in single atrial myocytes 5 min after cell membrane rupture at stimulation frequencies between 0.2 and 4 Hz. 40–50 stimuli were applied to achieve steady state conditions. The resting membrane potential (RMP) was corrected for the junction potential, mean values were −76.3±2.2 mV (n=10) in SR and −78.9±2,9 mV in AF (n=8, p=ns vs. SR). AP amplitudes at 1 Hz averaged 116±3 mV (n=10) in SR and 120±2 mV (n=8;

Table 2
Composition of bath and pipette solutions

Current	Action potentials	I_{Ca}	I_{Na}
	I_{to}, I_{sus}, I_{K1}, I_{KACh}		
Bath solution (mM)	NaCl 136, KCl 5.4, $CaCl_2$ 2.0, $MgCl_2$ 1.0, NaH_2PO_4 0.33, HEPES 5, Glucose 10	CholineCl 136, CsCl 5.6, $CaCl_2$ 2.0, $MgCl_2$ 1.0, NaH_2PO_4 0.33, HEPES 5, Glucose 10	CsCl 132.5, NaCl 5.0, $MgCl_2$ 1.0, $CaCl_2$ 1.0, HEPES 20, Glucose 11
Pipette solution (mM)	KCl 20, K-aspartate 110, MgCl 1.0, HEPES 10, EGTA 5, Mg_2ATP 5, GTP 0.1, phosphocreatine 5	CsCl 20, Cs aspartate 110, HEPES 10, EGTA 10, MgCl 1.0, Mg_2ATP 5, GTP 0.1, phosphocreatine 5	CsF 135, NaCl 5.0, HEPES 5, EGTA 10, Mg_2ATP 5

p=ns vs. SR) in AF. Fig. 1 shows typical AP recorded from an SR (Fig. 1A) and from an AF cell (Fig. 1B). In SR, the AP duration (APD) is much longer at all frequencies and the cell displays a clear frequency dependent adaptation of the APD with a shortening at higher stimulation rates. In contrast, in AF, the APD is already very short at slow rates and there is almost no further shortening as the stimulation frequency is increased, rather, the AP at 1, 2 and 4 Hz are overlapping (Fig. 1B). The APD_{90} was greatly reduced in AF as illustrated in Fig. 1C. At 0.2 Hz, the APD_{90} was 319±48 ms in SR vs. 134±12 ms in AF, at 1 Hz, 255±45 ms vs. 104±9 ms and at 4 Hz, 213±26 ms vs. 98±8 ms ($p<0.001$ vs. SR for all frequencies)

3.2. Effects of AF on potassium currents

In Fig. 2, representative recordings of steady-state currents from a cell of an SR patient and a cell of an AF patient are displayed. Currents were recorded under conditions designed to eliminate I_{Na} and I_{Ca} as described in the figure legend. Steady-state current densities are presented in Fig. 2C. The presence of AF was associated with a significant increase in inward currents at hyperpolarizing test potentials, representing the inward component of the

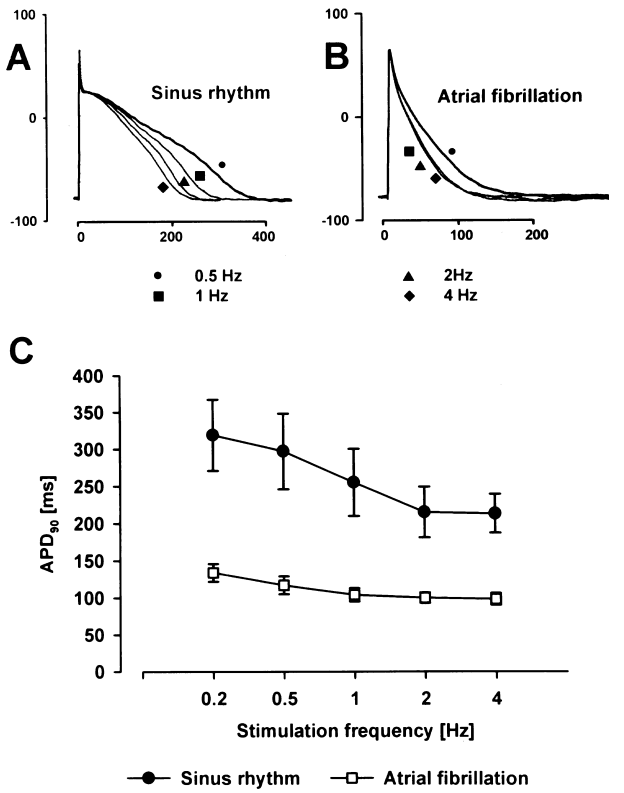

Fig. 1. AP recorded at 36°C from a human atrial cell of an SR patient (Panel A) and an AF patient (Panel B) at different stimulation frequencies. The units on the x-axis are ms, and mV on the y-axis. In Panel C, the AP duration to 90% repolarization (APD_{90}) from 10 cells of the SR and 8 cells of the AF group is shown as a function of the stimulation frequency.

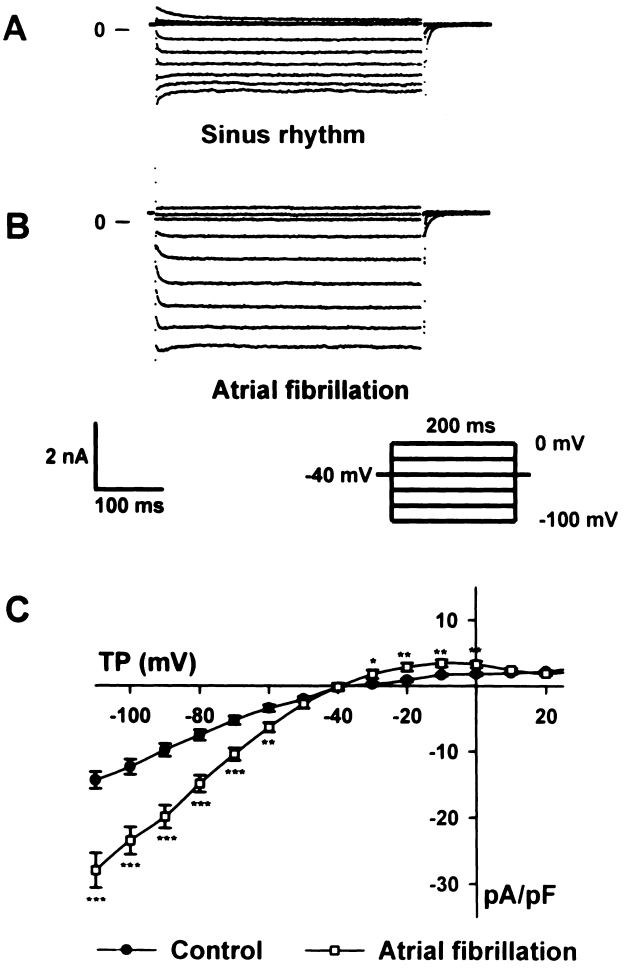

Fig. 2. Representative examples of steady-state current recordings in a human atrial cell from an SR patient (A) and from an AF patient (B). Currents were recorded at 36°C with 200 ms steps from a holding potential of −40 mV to test potentials between −100 mV and +20 mV. Stimulation frequency was 0.1 Hz and sustained currents were measured as current amplitudes at the end of the 200 ms test pulse. 1 μmol/l nisoldipine were added to the superfusion solution to block $I_{Ca,L}$. **0** indicates 0 current level. C: Steady-state current densities in SR and AF. n=43 for SR and 35 for AF, *$p<0.05$, **$p<0.01$, ***$p<0.001$ vs. SR.

inward rectifier potassium current (I_{K1}). For example, at −90 mV current densities averaged −9.83±0.96 pA/pF in SR and −19.91±1.72 pA/pF in AF ($p<0.001$). AF cells displayed increased outward currents at test potentials between −30 and 0 mV. For a test potential of −20 mV, current densities were 0.85±0.24 pA/pF in SR and 2.85±0.63 pA/pF in AF ($p<0.01$). At potentials positive to 0 mV, there were identical current densities in both groups. The reversal potential was not altered by AF: mean values were −36.7±3.6 mV in SR and −39.1±3.2 mV in AF (p=ns).

I_{KACh} was studied after addition of 1 μmol/l acetylcholine (ACh) to the bath solution (Fig. 3). In both groups, ACh led to an increase in current amplitudes. Current densities after ACh simulation were significantly larger in the AF group (Fig. 3C): mean I_{KACh} densities at −90 mV

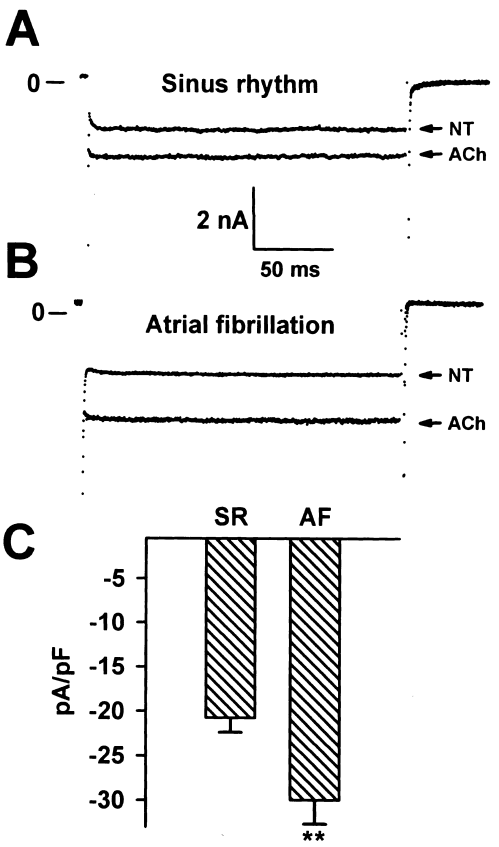

Fig. 3. I_{KACh} in human AF. I_{KACh} was recorded at 36°C with 200 ms test pulses to potentials between −60 and −120 mV, in 10 mV increments, from a holding potential of −40 mV. Panels A and B show the increase in potassium inward currents in response to 1 μmol/l acetylcholine in a cell from a patient in SR and from a patient in AF at a test potential of −90 mV. NT indicates the current in normal Tyrode's solution and ACh is the current measured after 10 min of superfusion with acetylcholine. 1 μmol/l nisoldipine were added to block $I_{Ca,L}$. C: Mean current densities at a TP of −90 mV for the SR (n=37) and for the AF (n=34) group. ** $p<0.01$ vs. SR.

were −20.7±1.6 pA/pF in SR and −30.0±2.7 mV in AF ($p<0.01$ vs. SR).

AF led to a marked reduction in I_{to} currents in human atrial cells. Typical cells from an SR and an AF patient are shown in Fig. 4. In SR, a large, transient, rapidly inactivating I_{to} is visible which is almost absent in AF. In contrast, I_{sus} at the end of the 200 ms test pulse had similar current amplitudes at positive potentials in both cells. I_{to} and I_{sus} were measured in 30 SR and in 15 AF cells. The current voltage (I–V) relations for I_{to} and I_{sus} are illustrated in Fig. 4C, D. I_{to} current densities were significantly reduced at all test potentials positive to 0 mV, i.e. at +50 mV from 7.84±0.76 pA/pF in SR to 1.24±0.28 pA/pF in AF ($p<0.001$ vs. SR), whereas I_{sus} current densities were identical in the 2 groups. The voltage dependence of I_{to} was assessed by expressing current amplitudes at a given voltage normalized to maximum current in each cell. The normalized I–V curves were shifted to more positive voltages in AF. To further evaluate the mechanism of a decreased I_{to}, we studied the voltage-dependent and kinetic properties (Table 3). Voltage-dependent activation was determined from the IV-relation with changes in driving force corrected by dividing the current during the test pulse (TP) by the driving force, TP−E_{rev}. E_{rev} is the reversal potential that was obtained as the reversal potential of I_{to} tail currents (−71.3 mV). The obtained curve was fit by a Boltzman relation. Voltage-dependent inactivation was determined with a 1s prepulse from a holding potential of −80 mV to potentials between −100 and +70 mV, followed by a 500 ms test pulse to +60 mV to record I_{to}. The obtained curve was fit by a Boltzman relation. AF was associated with a significant shift of I_{to} voltage-dependent activation to more positive potentials. Recovery from inactivation was assessed with a dual pulse protocol, in which two identical 300 ms pulses, P1 and P2, were applied from a holding potential of −80 mV to +50 mV at an increasing P1–P2-interval. The amplitude of P2 was normalized to the amplitude of P1. The recovery curve was best fit by a monoexponential function and was not altered by AF. I_{to} inactivation kinetics were determined by obtaining the inactivation time constant τ_{inact} from a monoexponential curve fit of the current decay during a depolarization to +50 mV. τ_{inact} was identical in the SR and in the AF group.

3.3. L-type calcium current

$I_{Ca,L}$ was studied 5 min after cell membrane rupture in all cells to avoid contaminating effects of $I_{Ca,L}$ rundown. Fig. 5 shows a typical example of calcium currents recorded from a cell of an SR and an AF patient. AF was associated with a marked decrease in $I_{Ca,L}$ amplitude. Fig. 5C shows the I–V relation for 42 cells in the SR and 18 cells in the AF group. The AF group had a highly significant decrease in $I_{Ca,L}$ current densities, for example at a test potential of +10 mV current densities were −6.97±0.50 pA/pF in SR and −1.88±0.19 pA/pF in AF ($p<0.001$ vs. SR). The voltage dependence of the current was not affected by AF, the normalized I–V relations were superimposed (Fig. 5D).

To evaluate the mechanisms involved in the reduction of $I_{Ca,L}$, we studied the voltage-dependent and kinetic properties of the current (Table 3). The voltage dependence of activation was assessed by dividing peak current at a given test potential by the driving force. The driving force was calculated as the difference between the test potential and the $I_{Ca,L}$ reversal potential which was determined from the I–V relation as the intercept with the x-axis of the ascending limb of the curve. The results were fit by a Boltzman relation. Voltage-dependent inactivation was obtained with a double pulse protocol with a 1 s inactivating prepulse to voltages between −100 and +40 mV from a HP of −80 mV, followed by a 200 ms test pulse to +10 mV. The currents were normalized to the maximum current and fit to a Boltzman relation. Both voltage-dependent

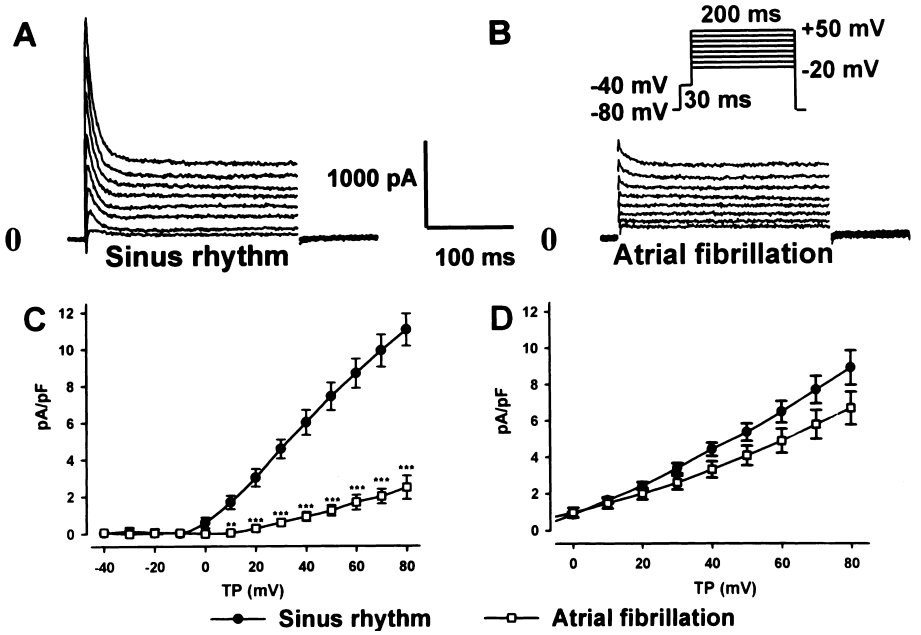

Fig. 4. Transient outward currents I_{to} at 36°C in human atrial cells were obtained with the pulse protocol shown in the inset. A 30 ms prepulse was used to inactivate I_{Na} and 1 μmol/l nisoldipine were added to the bath solution to inhibit $I_{Ca,L}$. In panel A, a cell from a patient in SR is shown, the recordings in panel B are from a patient in chronic AF. I_{to} was measured as the difference between peak outward current and the outward current at the end of the 200 ms test pulse. I_{sus} was the current amplitude at the end of the depolarizing step. **0** indicates 0 current level. C: I_{to} current densities. D: I_{sus} current densities. TP: Test potential. $^{**}p<0.01$, $^{***}p<0.001$ vs. SR.

activation and inactivation were not affected by AF. Recovery from inactivation was determined by the ratio of the current during a 300 ms depolarizing pulse to +10 mV (P2) from a HP of −80 mV to that during an identical conditioning pulse (P1) with a varying P1–P2 interval. Recovery was best fit by a monoexponential function and was identical in SR and in AF. In AF cells, the inactivation kinetics of calcium currents were slower than in SR. A

Table 3
Properties of I_{to}, I_{Ca} and I_{Na} in SR and in AF[a]

	I_{to}		I_{Ca}		I_{Na}	
	SR	AF	SR	AF	SR	AF
Voltage-dependent activation						
n	44	21	42	18	44	25
$V_{h,act}$ (mV)	18.7±0.6	34.6±0.8[b]	−0.1±1.6	−5.5±4.0	−50.2±0.2	−48.6±0.2
k_{act} (mV)	10.2±0.5	14.6±0.7	7.2±1.4	7.8±3.5	5.3±0.2	5.7±0.2
Voltage-dependent inactivation						
n	10	9	40	13	29	13
$V_{h,inact}$ (mV)	−40.3±0.9	−42.4±1.4	−24.7±0.3	−25.5±1.3	−97.2±0.3	−87.6±0.2[b]
k_{inact} (mV)	14.7±0.8	17.5±1.3	6.6±0.3	8.5±1.1	6.2±0.3	4.5±0.2[b]
Recovery from inactivation						
n	26	6	19	9	22	19
$\tau_{recover}$ (ms)	18.1±1.5	18.4±2.0	28.1±1.4	37.1±3.6	2.14±0.07	2.10±0.07
Kinetic properties						
n	12	7	39	16	13	10
Test potential (mV)	+50	+50	+10	+10	−35	−35
τ_{act} (ms)					0.30±0.03	0.47±0.05
τ_{fast} (ms)	13.39±1.81	14.61±2.69	5.1±0.6	8.3±0.9[b]	1.23±0.06	1.46±0.10
τ_{slow} (ms)			55.2±2.3	62.8±4.1		

[a] $V_{h,act}$ and $V_{h,inact}$: half-activation and half-inactivation voltages. k_{act} and k_{inact}: slope factors for activation and inactivation. $\tau_{recover}$: time constant of recovery from inactivation. τ_{act}: activation time constant, and τ_{fast} and τ_{slow}: fast and slow inactivation time constants.

[b] $p<0.01$ vs. SR.

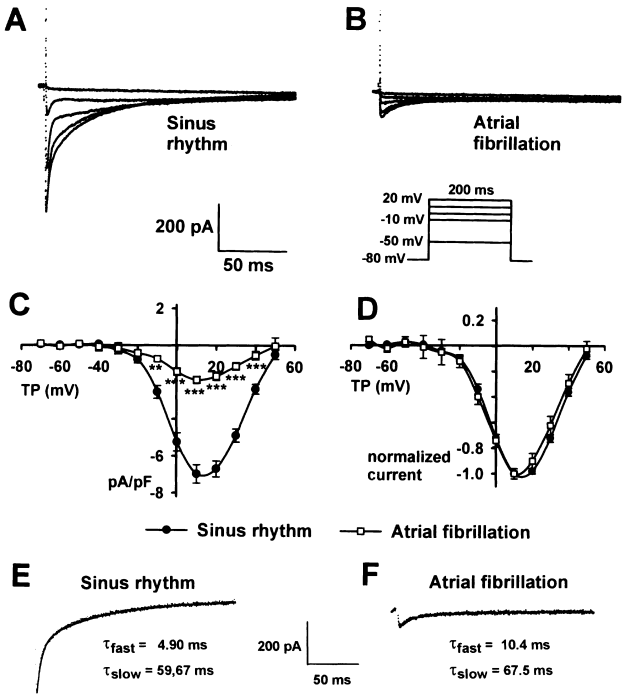

Fig. 5. Effects of AF on L-type calcium current in humans. Representative recordings from a cell of an SR patient (Panel A) and a cell from an AF patient (Panel B) are illustrated. Currents were recorded at 36°C with 200 ms depolarizing pulses to TP between −70 and +40 mV from a holding potential of −80 mV and a stimulation frequency of 0.1 Hz. In Panel C, current densities are plotted as a function of the test potential (TP). $^{**}p<0.01$, $^{***}p<0.001$ vs. SR. The voltage dependence of I_{Ca} was not altered by AF, shown in Panel D as an overlap of the curves when current amplitudes were normalized to the maximum current in each cell. E: I_{Ca} inactivation kinetics. Two representative traces of I_{Ca} recorded upon a depolarization to +10 mV are shown. Inactivation kinetics were analyzed by fitting a biexponential relation to the time course of current decay. The fit is shown as the solid line overlapping the current trace. The time constants τ_{fast} and τ_{slow} were obtained for each cell in that fashion. In the inset, the values for the fast and slow time constants are displayed. AF was associated with a slowing in I_{Ca} inactivation with a reduction of the fast time constant τ_{fast}.

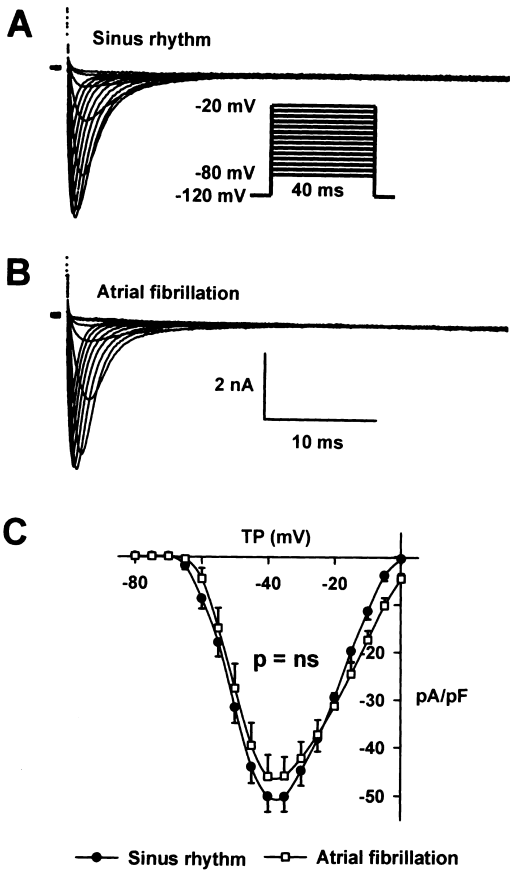

Fig. 6. Sodium current density in human atrium is not altered by AF. Representative recordings of sodium currents at room temperature are shown for an SR cell in Panel A and for an AF cell in Panel B. Currents were elicited from a HP of −140 mV with 40 ms depolarizing steps to TP between −80 and 0 mV. The intracellular and extracellular sodium concentration was 5 mmol/L. C: *I–V* relation of I_{Na} current densities.

typical example is shown in Fig. 5 Panels E, F. Cells from the AF group had a significantly longer fast time constant τ_{fast}, whereas τ_{slow} was not changed.

3.4. Sodium current

To avoid contaminating effects of time-dependent changes in the I_{Na} *I–V* relationship, all experiments were carried out 15 min after cell membrane rupture. Representative examples of I_{Na} recorded from an SR and an AF cell are shown in Fig. 6. Both cells had identical current amplitudes. Overall results for I_{Na} current densities are displayed in Fig. 6C. Neither current densities nor the voltage dependence of the current was altered by chronic AF in humans. Mean values at −40 mV were −50.2±3.1 pA/pF in SR (n=44) and −46.1±4.5 pA/pF in AF (n=25; p=ns vs. SR).

Voltage-dependent activation of I_{Na} was assessed by dividing current amplitudes by the driving force (the difference of the test potential and the reversal potential, which was obtained by the intercept of the ascending limb of the *I–V* relation with the *x*-axis). A double-pulse protocol at a HP of −140 mV was used to determine the voltage-dependent inactivation with a 1s conditioning pulse to voltages between −140 and −55 mV, followed by a 30 ms test pulse to −40 mV at 0.1 Hz. The test pulse current was then normalized to current without a prepulse and fit by a Boltzman relation. Voltage-dependent activation was not affected by AF (Table 3). Voltage-dependent inactivation of I_{Na} was shifted to more positive voltages in AF cells (Fig. 7), from −97.2±0.3 mV in SR to −87.6±0.2 mV in AF (p<0.01 vs. SR). The time-dependent recovery of I_{Na} was studied with the use of a double pulse protocol with two identical 30 ms pulses (P1 and P2) to −40 mV from a HP of −140 mV at an increasing P1–P2 interval. P2 amplitude was normalized to the amplitude of P1 and plotted as a function of the P1–P2 interval. Recovery kinetics were best fit by a monoexponential function and were not altered by AF. Activation and

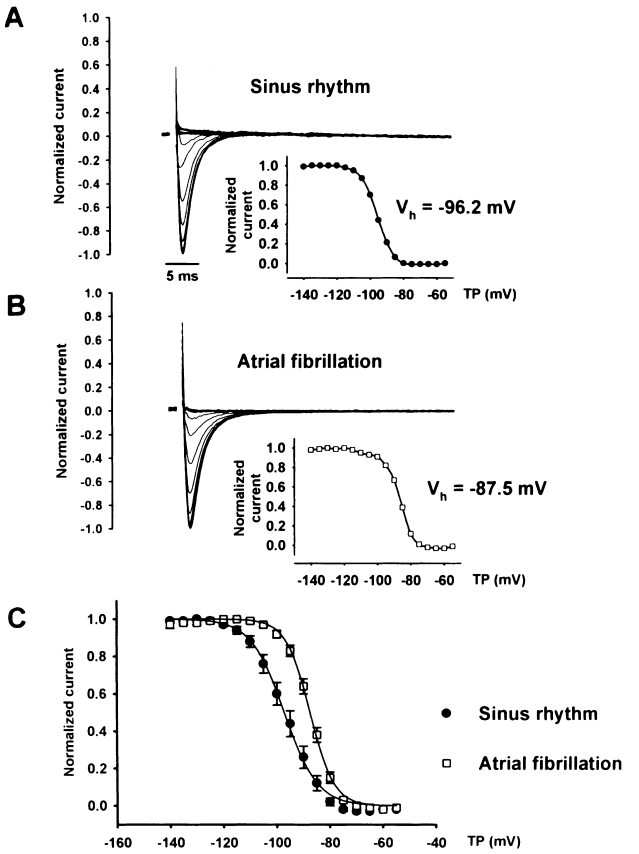

Fig. 7. I_{Na} voltage-dependent inactivation in SR and AF. Panels A and B illustrate typical examples of currents recorded with a double-pulse protocol. A 1 s conditioning pulse to voltages between −140 and −55 mV, from a HP of −140mV, was followed by a 30 ms test pulse to −40 mV. For reasons of clarity, only currents recorded with the test pulse are shown. In the inset, the inactivation curve is plotted as a function of the conditioning pulse potential for the respective cell. In Panel C, overall results for inactivation curves for the SR (n=29) and AF group (n=13) are shown. TP indicates the conditioning pulse potential. V_h is the half inactivation potential for I_{Na}.

inactivation kinetics were obtained by fitting a mono-exponential function to the activating and the inactivating portion of the current at a test potential of −35 mV. Neither activation nor inactivation kinetics were altered by AF.

4. Discussion

We have shown that chronic AF in humans leads to a marked shortening in atrial AP duration and to a decreased frequency-dependent adaptation of APD. Additionally, we have characterized the ionic mechanisms that underlie electrical remodeling in human AF. This study is the first to demonstrate that presence of the arrhythmia was associated with a marked decrease in $I_{Ca,L}$ in humans. Furthermore AF led to a decrease in I_{to} current densities as well as an increase in the steady-state outward current at potentials between −30 and 0 mV. These currents, therefore, seem to play a major role in the shortening of repolarization in AF. At hyperpolarizing potentials, we observed an increase in I_{K1} and in I_{KACh} current densities in AF. I_{Na} voltage-dependent inactivation was shifted to more positive potentials by AF in humans.

4.1. Comparisons with previous findings on the effect of AF on repolarization

We observed a decrease in APD and APD adaptation to rate in chronic human AF. These findings are consistent with previous reports about a shortening of atrial repolarization in vivo. In a goat model, Wijffels et al. [7] demonstrated that AF was associated with a shortening of the atrial ERP and a decreased ERP adaptation to rate. These findings were confirmed in three studies in the canine rapid atrial pacing model of AF [8–10]. In this model, Yue et al. [16] have also recorded AP where they found a progressive shortening of the APD and a decreased APD adaptation to rate with an increased duration of rapid pacing. Boutjidir et al. [14] studied the effect of chronic AF on ERP and AP in multicellular preparations of human atria. AF was associated with a marked shortening of the ERP and AP as well as an increased dispersion of repolarization. In a study that addressed the effects of short-term, pacing-induced AF in humans [12], a reversible shortening of atrial ERP was noted. A marked shortening of the ERP was also present in patients in chronic lone AF briefly after conversion to SR [11]. Our findings provide likely ionic mechanisms of shortened repolarization in AF with a decrease in $I_{Ca,L}$ and I_{to} current densities as well as an increase in steady-state outward current densities at potentials relevant to phase 3 of the atrial AP. $I_{Ca,L}$ is important in rate-dependent changes in human atrial APD [26]. Like in animal models [16], the observed reduction in $I_{Ca,L}$ in our study is the likely mechanism for a decrease in APD rate adaptation in AF.

4.2. Comparison with previous studies of ionic changes in atrial disease

Little is known about ionic changes in AF. The only report in humans by Van Wagoner et al. [18] showed a clear reduction in I_{to} current densities that was in the same order of magnitude as in the present study. A reduction in I_{to} current densities was involved in atrial electrical remodeling in the canine rapid pacing model [16].

In our study, I_{sus} current density was not different from patients in normal SR. This is in contrast to the study by Van Wagoner et al., who showed a decrease in I_{sus} current densities and a decreased Kv1.5 protein expression in human AF [18]. The reasons for these contrasting results may reflect differences in patients' underlying cardiac disease or in left ventricular function. Reduced left ventricular function and heart failure are known to alter electrophysiology and potassium currents in the atria [22,27,28]. Most of our patients had a preserved or only

mildly impaired left ventricular function. In the study of Van Wagoner et al. these data are not given, so differences in left ventricular function could account for the differences observed. Further reasons might include the duration of AF or the patients' medications. In the canine rapid pacing model, $I_{Kur,d}$, which underlies the sustained outward current in that species, was not altered by AF [16]. This current however, appears to have a different molecular basis than I_{Kur} in human atrium [29].

I_{K1} at hyperpolarizing potentials was increased in appendages from AF patients in the present study. This was also found in the report by Van Wagoner et al. [18], however, they observed an increase in left atrial myocytes only. In cells from the right atrium, I_{K1} was not affected by AF. In contrast, I_{K1} current densities were not altered in dogs subjected to rapid atrial pacing [16]. I_{KACh} was also substantially enlarged in our AF patients at hyperpolarizing potentials. We are not aware of any studies about the effects of AF on I_{KACh}. The current is important in contributing to the resting membrane potential and is involved in atrial APD shortening by acetylcholine [30]. Cholinergic modulation of atrial repolarization is largely based on the activation of I_{KACh} [30,31], and is associated with an increase in the heterogeneity of atrial repolarization [32,33]. Vagal stimulation facilitates the induction of AF in experimental models and an increased vagal tone seems to facilitate certain types of clinical AF [34,35]. It is therefore likely that changes in I_{KACh} current density or heterogeneous expression are important factors both in the induction and in the maintenance of AF.

In AF, $I_{Ca,L}$ current densities were reduced by 73% compared to SR. Similar reductions in $I_{Ca,L}$ were observed after chronic rapid atrial pacing in dogs [16,36] and in a preliminary report in humans [37]. In the dog model [36], like in our study, $I_{Ca,L}$ inactivation was slowed in AF cells, possibly contributing to a decreased Ca^{2+} influx especially at rapid rates.

Sodium current densities were identical in patients in SR and in AF in our study. These results contrast with observations that showed a progressive reduction in I_{Na} density as a function of atrial tachycardia in the dog [17]. Another preliminary report in the rapid pacing model also described a reduction in I_{Na} current densities, however, this was attributed to an increase in cell size, since current amplitudes remained unchanged [36]. The reasons for these contrasting results might include differences in the type of AF (experimental vs. clinical AF), influences of the underlying cardiac disease or interspecies differences. In our AF group, voltage-dependent inactivation of I_{Na} was shifted by 9.6 mV to more positive potentials, which would increase availability at the resting potential, and thus increase conduction velocity. Therefore, other mechanisms must be involved in the slowing of intraatrial conduction in AF. Several studies have investigated the effects of AF on atrial gap junctions, which are a major determinant in myocardial conduction [38,39]. Elvan et al. [40] found an increase in connexin 43 (Cx43) protein expression as well as a redistribution of the protein towards the lateral sides of the myocytes in experimental AF in dogs. In contrast, van der Velden et al. [41] did not observe a change in Cx43 mRNA or protein expression, but a redistribution of Cx40 expression in the AF goat model. In human AF, Cx43 protein expression was reduced compared to SR [42]. Although the results about the exact changes in gap junctions are still contrasting, altered intercellular coupling seems to be an important component in the remodeling process in AF. These changes might overcompensate the AF-associated shift in voltage-dependent inactivation of I_{Na}, thereby causing an overall slowing of intraatrial conduction in AF.

4.3. Potential mechanisms by which AF changes ionic currents

Few data are available upon the mechanisms by which AF alters cardiac ionic currents. In the present report, half-maximal activation of I_{to} was shifted to more positive voltages. However, this shift is not sufficient to account for the total reduction of I_{to}, because maximal I_{to} conductance was decreased, (i.e. at $+50$ mV: 1.46 ± 0.15 μS in SR and 0.46 ± 0.11 μS in AF). Therefore, other mechanisms seem to be involved in the downregulation of I_{to}. Yue et al. have reported, with the canine rapid pacing model, a decrease in Kv4.3 mRNA after 42 days of rapid atrial pacing [43] which is in the same range as the current reduction observed in our AF patients. In the same study, the authors also observed a downregulation of the L-type calcium channel α1c-subunit in chronically paced dogs [43]. In one preliminary report in humans, the $I_{Ca,L}$ α1-subunit was decreased in AF lasting more than 6 months, but not in short-term AF [44].

4.4. Potential limitations

In human atrial appendages, the chunk method is the only possibility of cell isolation. The use of this method has important implications on the results obtained in single human atrial cells. 1) Yue et al. [45] provided evidence that I_K is present in a much smaller percentage of cells with smaller current amplitudes if the chunk method is used for cell isolation compared to arterial cannulation. In our preparations, I_K was present only in a small number of cells ($<5\%$) with very small current amplitudes. Most of the time, the current displayed rapid rundown, so a comparison between different groups or a systematic pharmacological approach was not possible. 2) We observed an increase in I_{K1} and in I_{KACh} in the AF group. As both currents are important contributors to the maintenance of the resting membrane potential (RMP), a more negative value would be expected in AF. However, in isolated human atrial cells the RMP is highly variable, which again seems to be a consequence of the isolation procedure. For

the recording of AP, only cells with a very good RMP were eligible. Consequently, RMP and AP were measured in a highly-selected cell population which may not be representative. Although the RMP had a more negative value in the AF group, the difference was not statistically significant. 3) We have demonstrated a marked shortening of the APD in AF. AP in SR cells had a duration similar to those previously described for AP in multicellular preparations [14] and for the ERP in vivo [11]. In contrast, our APD in isolated AF cells were shorter than AP or ERP in these studies. This might reflect a different suspectibility of currents to the isolation procedure in AF and may have contributed to the marked shortening of repolarization in our study.

I_{Na} was recorded at room temperature and with an external Na concentration of 5 mmol/l. These unphysiological conditions might have affected the I_{Na} recordings and may have contributed to the differences observed in the two groups.

4.5. Potential significance

Although rapid progress in defining the electrophysiological substrates of AF has been made over the last few years [7–12], the clinical management of AF is still limited by low efficacy or severe adverse events of current therapeutic approaches [46]. The present study is the first to demonstrate the effects of chronic AF on repolarization in isolated human atrial cells. We have also defined the ionic changes underlying altered repolarization in this arrhythmia. The understanding of these mechanisms may have an important impact on the development of new pharmacological or non-pharmacological therapies. These could include the modulation of specific molecular targets to prevent or to reverse electrophysiological changes that allow the induction or the maintenance of AF. Our results warrant further investigation on the mechanisms involved in ionic current remodeling, namely studies on the regulatory functions of ion channels, differences in regional distribution as well as channel expression on the transcriptional and post-transcriptional level.

5. Conclusions

We have demonstrated that chronic AF in man is associated with a marked shortening and an impaired rate adaptation of repolarization in single atrial myocytes. The arrhythmia leads to important changes in ionic currents that determine atrial repolarization. These include a significant decrease in $I_{Ca,L}$ and I_{to}, as well as an increase in the steady-state outward current at potentials relevant during phase 3 of the AP. Furthermore, I_{K1} and I_{KACh} are increased at hyperpolarizing potentials. The understanding of the mechanisms underlying electrical remodeling in AF are crucial for the development of more efficient and less harmful therapeutic approaches to the arrhythmia.

Acknowledgements

This study was supported by the Bundesministerium für Bildung und Forschung (BMBF-DLR 01EC 9405), by the Franz-Loogen-Stiftung and by the Dr. Karl-Kuhn-Stiftung. The authors thank Dr. Stanley Nattel for editorial comments.

References

[1] Kannel WB, Abbott RD, Savage DD, McNamara PM. Epidemiologic features of chronic atrial fibrillation: the Framingham study. N Engl J Med 1982;306:1018–1022.
[2] The National Heart La. Atrial fibrillation. Current understandings and research imperatives. J Am Coll Cardiol 1993;22:1830–1834.
[3] Halperin JL, Hart RG. Atrial fibrillation and stroke: new ideas, persisting dilemmas. Stroke 1988;19:937–941.
[4] Wolf PA, Dawber TR, Thomas HE, Kannel WB. Epidemiologic assessment of chronic atrial fibrillation and risk of stroke: the Framingham study. Neurology 1978;28:973–977.
[5] Cairns JA, Connelly SJ. Nonrheumatic atrial fibrillation: risk of stroke and antithrombotic therapy. Circulation 1991;84:469–481.
[6] Krahn AD, Manfreda J, Tate RB, Mathewson FAL, Cuddy TED. The natural history of atrial fibrillation: incidence, risk factors, and prognosis in the Manitoba follow-up study. Am J Med 1995;98:476–484.
[7] Wijffels MCEF, Kirchhof CJHJ, Dorland R, Allessie MA. Atrial fibrillation begets atrial fibrillation: a study in awake, chronically instrumented goats. Circulation 1995;92:1954–1968.
[8] Morillo CA, Klein GJ, Jones DL, Guiraudon CM. Chronic rapid atrial pacing: structural, functional and electrophysiological characteristics of a new model of sustained atrial fibrillation. Circulation 1995;91:1588–1595.
[9] Gaspo R, Bosch RF, Talajic M, Nattel S. Functional mechanisms underlying tachycardia-induced sustained atrial fibrillation in a chronic dog model. Circulation 1997;96:4027–4035.
[10] Elvan A, Wylie K, Zipes DP. Pacing-induced chronic atrial fibrillation impairs sinus node function in dogs – Electrophysiological remodeling. Circulation 1996;94:2953–2960.
[11] Kumagai K, Akimitsu S, Kawahira K et al. Electrophysiological properties in chronic lone atrial fibrillation. Circulation 1991;84:1662–1668.
[12] Daoud EG, Bogun F, Goyal R et al. Effects of atrial fibrillation on atrial refractoriness in humans. Circulation 1996;94:1600–1606.
[13] Misier AR, Opthof T, van-Hemel NM et al. Increased dispersion of ''refractoriness'' in patients with idiopathic paroxysmal atrial fibrillation. J Am Coll Cardiol 1992;19:1531–1535.
[14] Zhang S, Sawanobori T, Hirano Y, Hiraoka M. Multiple modulations of action potential duration by different calcium channel blocking agents in guinea pig ventricular myocytes. J Cardiovasc Pharmacol 1997;30:489–496.
[15] Allessie MA. Reentrant mechanisms underlying atrial fibrillation. In: Zipes DP, Jalife J, editors, Cardiac electrophysiology – From cell to bedside, Philadelphia: Saunders, 1995, pp. 562–566.
[16] Yue L, Feng J, Gaspo R et al. Ionic remodeling underlying action potential changes in a canine model of atrial fibrillation. Circ Res 1997;81:512–525.
[17] Gaspo R, Bosch RF, BouAbboud E, Nattel S. Tachycardia-induced

changes in Na^+ current in a chronic dog model of atrial fibrillation. Circ Res 1997;81:1045–1052.
[18] Van Wagoner DR, Pond AL, McCarthy PM, Trimmer JS, Nerbonne JM. Outward K^+ current densities and Kv1.5 Expression are reduced in chronic human atrial fibrillation. Circ Res 1997;80:772–781.
[19] Escande D, Coulombe A, Faivre JF, Deroubaix E, Corabouef E. Two types of transient outward currents in adult human atrial cells. Am J Physiol 1987;252:H142–H148.
[20] Wang Z, Fermini B, Nattel S. Sustained depolarization-induced outward current in human atrial myocytes. Evidence for a novel delayed rectifier K^+ current similar to Kv1.5 cloned channel currents. Circ Res 1993;73:1061–1076.
[21] Fedida D, Wible B, Wang Z et al. Identity of a novel delayed rectifier current from human heart with a cloned K^+ channel current. Circ Res 1993;73:210–216.
[22] Koumi SI, Backer CL, Arentzen CE. Characterization of inwardly rectifying K^+ channel in human cardiac myocytes. Circulation 1995;92:164–174.
[23] Heidbüchel H, Vereecke J, Carmeliet E. The electrophysiological effects of acetycholine in single human atrial cells. J Mol Cell Cardiol 1987;19:1207–1219.
[24] Bosch RF, Milek IV, Popovic K et al. Ambasilide prolongs the action potential and blocks multiple potassium currents in human atrium. J Cardiovasc Pharmacol 1999;289:156–165.
[25] Gotoh Y, Imaizumi Y, Watanabe M et al. Inhibition of transient outward K^+ current by DHP Ca^{2+} antagonists and agonists in rabbit cardiac myocytes. Am J Physiol 1991;260:H1737–H1742.
[26] Li GR, Nattel S. Properties of human atrial ICa at physiological temperatures and relevance to action potential. Am J Physiol 1997;272:H227–H235.
[27] Wang YG, Schreieck J, Weyerbrock S, Overbeck M, Meisner H. Unterschiedlicher transienter Auswärtsstrom (Ito) in atrialen Kardiomyozyten von Patienten mit und ohne Herzinsuffizienz. Z Kardiol 1998;87:125, (Abstract).
[28] Wegener JW, Nawrath H. Action of tertiary phenylalkylamines on cardiac transient outward current from outside the cell membrane. Naunyn Schmiedebergs Arch Pharmacol 1996;354:746–754.
[29] Yue L, Feng J, Li GR, Nattel S. Characterization of an ultrarapid delayed rectifier potassium channel involved in canine atrial repolarization. J Physiol Lond 1996;496:647–662.
[30] Zaza A, Malfatto G, Schwartz PJ. Effects on atrial repolarization of the interaction between K^+ channel blockers and muscarinic receptor stimulation. J Pharmacol Exp Ther 1995;273:1095–1104.
[31] Visentin S, Wu SN, Belardinelli L. Adenosine-induced changes in atrial action potential: contribution of Ca- and K-currents. Am J Physiol 1990;258:H1070–H1078.
[32] Allessie R, Nusynowitz M, Abildskov JA, Moe GK. Non-uniform distribution of vagal effects on atrial refractory period. Am J Physiol 1958;194:406–410.
[33] Allessie MA, Lammers WJ, Bonke IM, Hollen J. Intra-atrial reentry as a mechanism for atrial flutter induced by acetylcholine and rapid pacing in the dog. Circulation 1984;70:123–135.
[34] Coumel P. Role of the autonomic nervous system in paroxysmal atrial fibrillation. Clin Cardiol 1990;13:209–212.
[35] Waxman MB, Cameron DA, Wald RW. Interactions between the autonomic nervous system and supraventricular tachycardia in humans. In: Zipes DP, Jalife J, editors, Cardiac electrophysiology: from cell to bedside, Philadelphia: W.B. Saunders Company, 1995, pp. 699–722.
[36] Pu J, Shvilkin A, Hara M, Danilo P, Boyden PA. Altered inward currents in myocytes from chronically fibrillating canine atria. Circulation 1997;96:1–180 (abstract).
[37] Van Wagoner DR, Lamorgese M, Kirian P. Calcium current density is reduced in atrial myocytes isolated from patients in chronic atrial fibrillation. Circulation 1997;96:1–180 (abstract).
[38] Pressler M, Munster P, Huang CD. Gap junction distribution in the heart: functional relevance. In: Zipes D, Jalife J, editors, Cardiac electrophysiology: from cell to bedside, Philadelphia, PA: W.B. Saunders, 1995, pp. 144–151.
[39] Spach MS, Starmer CF. Altering the topology of gap junctions, a major therapeutic target for atrial fibrillation. Cardiovasc Res 1995;30:337–344.
[40] Elvan A, Huang XD, Pressler ML, Zipes DP. Radiofrequency catheter ablation of the atria eliminates pacing-induced sustained atrial fibrillation and reduces connexin 43 in dogs. Circulation 1997;96:1675–1685.
[41] van derVelden HMW, van Kempen MJA, Wijffels MCEF et al. Altered pattern of connexin40 distribution in persistent atrial fibrillation in the goat. J Cardiovasc Electrophysiol 1998;9:596–607.
[42] Patel P, Jones DG, Dupont E. Remodelling of atrial connexin43 expression in human atrial fibrillation. Eur Heart J 1998;19:465, (Abstract).
[43] Yue L, Wang Z, Gaspo R, Nattel S. The molecular mechanism of ionic remodeling of repolarization in a dog model of atrial fibrillation. Circulation 1997;96:1–180 (abstract).
[44] Brundel BJ, Van Gelder IC, Hennings RH. Downregulation of the mRNA expression of L-type calcium channel and acetylcholine-activated potassium channel in chronic atrial fibrillation. Eur Heart J 1997;18:193 (abstract).
[45] Yue L, Feng J, Li GR, Nattel S. Transient outward and delayed rectifier currents in canine atrium. properties and role of isolation methods. Am J Physiol 1996;270:H2157–H2168.
[46] Nattel S, Hadjis T, Talajic M. The treatment of atrial fibrillation. An evaluation of drug therapy, electrical modalities and therapeutic considerations. Drugs 1994;48:345–371.